
Proceedings Paper:
Kudryavtsev, V.A. (2018) Cosmogenic Activation: Recent Results. In: Low Radioactivity Techniques 2017 (LRT 2017). 6th International Workshop on Low Radioactivity Techniques, 23-27 May 2017, Seoul, Korea. AIP Conference Proceedings, 1921 . AIP Publishing . ISBN 978-0-7354-1613-0

https://doi.org/10.1063/1.5022583

Cosmogenic activation: Recent results

Vitaly A. Kudryavtsev

Citation: AIP Conference Proceedings **1921**, 090004 (2018); doi: 10.1063/1.5022583
View online: https://doi.org/10.1063/1.5022583
View Table of Contents: http://aip.scitation.org/toc/apc/1921/1
Published by the American Institute of Physics

Cosmogenic Activation: Recent Results

Vitaly A. Kudryavtsev

Department of Physics and Astronomy, University of Sheffield, Hounsfield Road, Sheffield, UK

v.kudryavtsev@sheffield.ac.uk

Abstract. Activation of materials is known to cause background events in underground experiments that may affect the sensitivity of these experiments to rare event searches. The most common source of activation is the exposure of materials to cosmic rays at the surface of the Earth but other various sources of neutrons may also be dangerous. Different computer codes provide estimates of production rates of radioactive isotopes due to activation but their results are sometimes inconsistent. High-sensitivity experiments looking for dark matter, neutrino-less double-beta decay or neutrinos from various sources, although affected by activation, provide crucial tests of models used in the codes. Recent calculations and measurements of activation rates are discussed in this paper.

INTRODUCTION

Activation is the process of production of radioactive isotopes in materials by nuclear transmutation caused by natural or artificial radiation. A typical example of activation is the exposure of materials to cosmic rays at surface of the Earth or at higher altitudes. All materials located above ground are exposed to cosmic rays and, hence, may be activated. Subsequent decays of radioactive isotopes produce by activation, contribute to the background radiations that we observe at the surface or in any protected environment. Other examples include activation by radioactive sources and cosmic-ray muon component underground.

The activation does not pose any threat to human beings as we are exposed to cosmic rays ourselves without any damaging consequences, being protected from the high flux of primary cosmic rays by the Earth atmosphere. However, certain experiments requiring ultra-low background conditions may suffer from cosmic-ray activation if measures are not taken to suppress or reject background events caused by activated materials. The main contribution to the background rate from activated materials come from the isotopes that have lifetimes ranging from a few hours to a few years. Radioactive isotopes with very short lifetimes (about a few seconds or less) can be tracked in a detector and candidate signal events linked to the decays of these isotopes in time or/and in space, can be removed from further analysis. (These time/space coincidences can also be used to understand the background from activation on-site.) Longer lifetimes, but still with a few days or weeks, are still short enough and a waiting time of a few weeks or months after moving the detector in a protected environment (i.e. underground) or removing an artificial source (neutron calibration source, for instance), will lead to the decay of most radioactive atoms. Isotopes with very long lifetimes (more than a few years), will have the decay rates (inverse proportional to lifetimes) quite low to pose a threat to the high-sensitivity experiment.

The problem of background radiations due to activation has been reviewed in Refs. [1, 2, 3]. In this paper I describe recent developments in modelling and measuring the production and decay rates of radioactive isotopes from material activation with an emphasis on materials used in ultra-low background underground experiments for dark matter and neutrino-less double-beta decay searches, and low-energy neutrino detection.

ACTIVATION PROCESS

The production rate of radioactive isotopes can be calculated using the equation:

$$R = \int_0^\infty \sigma(E) \frac{dF}{dE}(E) dE, \tag{1}$$

Low Radioactivity Techniques 2017 (LRT 2017)
AIP Conf. Proc. 1921, 090004-1–090004-6; https://doi.org/10.1063/1.5022583
Published by AIP Publishing. 978-0-7354-1613-0/$30.00

where $\sigma(E)$ is the energy dependent cross-section of the production of a particular isotope in a material and $\frac{dF}{dE}(E)$ is the energy spectrum of particles causing the activation. The equation above is just a simple example of activation of a material consisting of only one element with only one stable isotope. In reality, most materials are composed of several elements, each containing one or more stable isotopes. In this case, to estimate the production of a particular isotope, a sum over all isotopes present in the material should be calculated. This is what is usually returned by the codes evaluating production rates.

For calculation of activation of materials at the surface of the Earth, the energy spectrum of cosmic rays at a particular location should be used. Since the production of radioactive isotopes (as well as any isotopes) requires nuclear transmutation, hadrons are the main contributors to this process. It is known that the total flux of cosmic rays on the surface of the Earth is dominated by muons but the flux of hadrons, in particular neutrons, is not negligible (a few percent of the total flux [4]) and, given the much higher cross-section of nuclear reactions initiated by hadrons compared to muons or photons, the main contribution to activation at the surface of the Earth comes from neutrons.

The parameter that is measured in the experiments is the decay rate of the activated isotope and the link between the decay rate and production rate is defined by:

$$\frac{dN}{dt} = R\left(1 - \exp\left(\frac{t_{exp}}{\tau}\right)\right)\exp\left(\frac{t_{dec}}{\tau}\right), \tag{2}$$

where $\frac{dN}{dt}$ is the decay rate of a radioactive isotope, R is the production rate of this isotope defined by Eq. (1), t_{exp} is the time during which a material was exposed to the radiation (cosmic rays at the surface of the Earth), t_{dec} is the cooling down time, i. e. the time during which the material was stored in a location without being irradiated and τ is the lifetime of the radioactive isotope.

If the irradiation (or exposure) time, t_{exp}, is much bigger than the lifetime τ of the radioactive isotope, whereas the cooling down time, t_{dec}, in Eq. (2) is very small compared to τ, then the decay rate is in equilibrium with the production rate $\frac{dN}{dt} \approx R$ and the latter can be measured directly. If the cooling down time is known then evaluating the production rate from the measured decay rate is straightforward as long as $t_{exp} >> \tau$. If the latter condition does not hold, the history of exposure of the material to cosmic rays should be known to evaluate production rate from the measurements. The procedure is even more complicated when the material is stored at different locations, at an elevated site compared to sea level, at high latitude, or transported by airplane. Another complication may arise from the chain of the decays if the initially produced isotope decays into an unstable nuclide.

CALCULATION OF PRODUCTION RATES

Several computer codes exist for calculation of production rates using Eq. (1). They use different cross-sections for production of isotopes in materials and different spectra of incident particles. For activation of materials by cosmic rays at the sea level, the measured or calculated neutron spectra can be used. A number of parameterisations have been suggested for neutron spectra at the surface of the Earth. The recent version of the ACTIVIA code [5] offers two options: the default parameterisation of neutron energy spectrum from Refs. [6, 7] and the parameterisation based on the recent measurements reported in Ref. [8]. These two spectra are different which obviously results in different neutron production rates. Neutron flux from Ref. [8] is higher than that from Refs. [6, 7] at energies below 2 GeV and drops quicker above 2 GeV (see [9, 10] for comparison).

Other available options include a parameterisation by Ziegler [11] based on multiple neutron flux measurements, and the spectra generated by the code CRY [12]. CRY generates various particles using pre-simulated (using MCNPX) distributions of these particles in atmospheric showers. Based on full Monte Carlo of atmospheric showers, CRY has an advantage over parameterisations by generating energy, angles and positions of different types of particles at 3 different heights in the atmosphere. However, it takes into account only primary protons (atmospheric showers from primary nuclei were not simulated) and has very wide bins in decimal logarithm of energy which reduces the accuracy of the spectra. Figure 1 [13] compares the neutron spectra from CRY with the two parameterisations given in Ref. [11] and Ref. [8].

All spectra discussed above refer to the sea level and to the location of the New York City. For different latitude, longitude and, in particular altitude, the neutron flux will be different. The flux also depends on the time within the solar modulation cycle. The shape of the spectrum above 10 MeV is not affected by the flux variation due to these factors. Corrections for different locations have been suggested in Ref. [11] and Ref. [8]. The web-site http://seutest.com/cgi-bin/FluxCalculator.cgi offers a nice tool in calculating such corrections. Figure 2 (left) [13] shows the neutron spectra

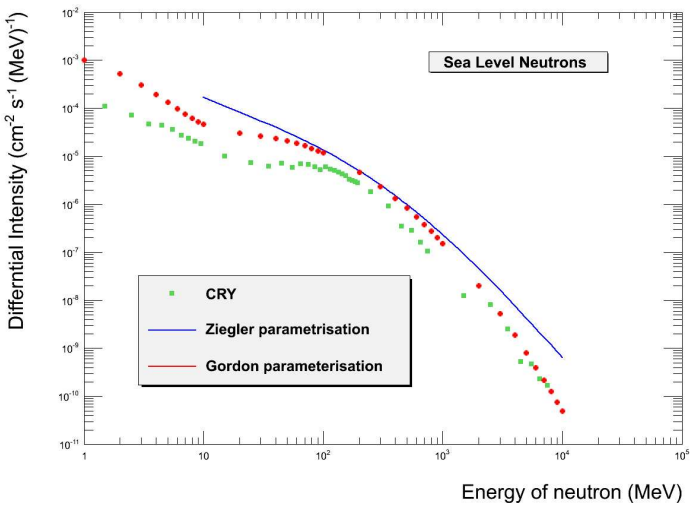

FIGURE 1. Neutron spectra from CRY [12] and parameterisations from Ref. [11] and Ref. [8].

from CRY at two different altitudes sea level and 2100 m above sea level. The spectral shapes are very similar implying that to the first approximation the altitude correction can be applied to the total high-energy neutron flux.

The 2nd largest hadronic component at sea level is the proton flux. Figure 2 (right) [13] shows the proton spectra from CRY at two different altitudes. By comparing the two figures (left and right) we can conclude that the neutron flux largely dominates (by about an order of magnitude) over the proton flux at neutron energies below a few GeV whereas at higher energies the two fluxes are approximately equal with possibly a slightly higher proton flux. The depletion of protons at low energies can be explained by their energy loss due to ionisation and atom excitation. Since the main production of isotopes occurs at energies of incident particles below a few GeV, neutron contribution is much more significant and the production of radioisotopes by protons is small.

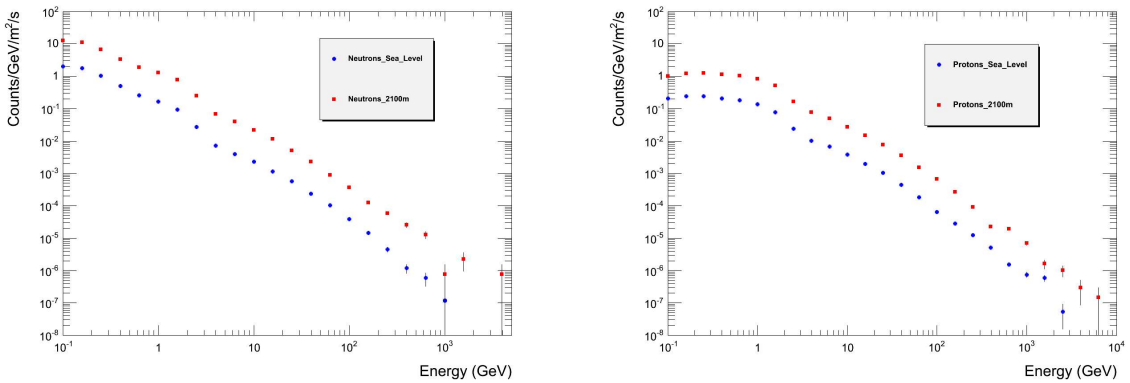

FIGURE 2. Energy spectra of neutrons (left) and protons (right) from CRY [12] at sea level and 2100 m above sea level [13].

The 2nd input to the calculation of the isotope production rates is the cross-section of nuclear reactions leading to the transmutation of nuclei. The ACTIVIA code [5] offers an option of using either semi-empirical formulae from Refs. [14, 15] or evaluated nuclear data libraries for medium energies MENDL-2/2p [16, 17]. An older COSMO code [18] provides the semi-empirical cross-sections from Ref. [14]. Among other possible cross-section libraries, it is worth mentioning TENDL library provided by the TALYS code [19] and ENDF library used in GEANT4 [20].

A comparison between different cross-section libraries and measurements have been shown in Refs. [1, 2, 3]. Recently published analysis of activation [10] included a comparison between the default cross-sections in ACTIVIA (pa-

TABLE 1. Calculated and measured production rates of radioactive isotopes in copper at sea level. The rates are given in kg^{-1} day^{-1}. The results for LNGS [22] have been scaled down to the sea level by a factor of 2.4 as suggested in [22]. The 3 columns for GEANT4 show separate contributions from neutrons and protons, and the total rate. The total includes also a small contribution from muons (not shown separately, as being much smaller than that from protons). The two columns for ACTIVIA show calculations with two neutron spectra: from Refs. [6, 7] and from Ref. [8]. In both cases the default semi-empirical cross-sections have been used.

Isotope	Half-life	GEANT4			ACTIVIA		COSMO	TALYS	Data	Data
	days	Neutrons	Protons	Total	[6, 7]	[8]	[18]	[21]	[22]	[23]
$^{46}_{21}$Sc	83.8	1.05	0.12	1.19	3.13	4.09	1.47		1.9 ± 0.6	2.3 ± 0.9
$^{54}_{25}$Mn	312.3	11.7	0.55	12.3	14.3	30.0	13.5	16.2	7.7 ± 0.8	13 ± 3
$^{59}_{26}$Fe	44.5	8.56	0.18	8.77	4.24	10.5	4.3		16 ± 4	4.1 ± 1.3
$^{56}_{27}$Co	77.3	9.71	0.54	10.32	8.74	20.1	7.0		8.3 ± 1.1	9.3 ± 1.3
$^{57}_{27}$Co	271.8	64.3	2.55	67.2	32.4	77.5	30.2	56.2	65 ± 14	45 ± 1.3
$^{58}_{27}$Co	70.9	55.5	1.57	57.3	56.6	138	22.7		59 ± 8	69 ± 5
$^{60}_{27}$Co	1925.28	63.1	1.25	64.6	26.3	66.1	25.7	46.4	76 ± 7	29 ± 6

rameterisations from Refs. [14, 15]) with TENDL-2014 (from TALYS [19]) and with cross-sections used in GEANT4. A reasonable agreement has been observed between GEANT4 and TENDL-2014 libraries whereas semi-empirical formulae used in ACTIVIA are different from GEANT4 or TENDL-2014 for most isotopes. It is not a surprise then that the production rates obtained with different codes are not in agreement for a large number of radioactive isotopes.

Note that parameterisations provided in Refs. [14, 15], as well as MENDL-2p library [17] provide proton-induced cross-sections, whereas the activation is dominated by neutron-induced reactions. Usually the charge independence is assumed to convert proton cross-section into the neutron one for high energies. However, the reaction products are not the same for the two type of reactions and it is not clear how these differences are dealt with in the codes.

COMPARISON WITH MEASUREMENTS

The crucial test of the calculation of production rates is the comparison with measurements. As an example, Table 1 shows the calculations and measurements of the production rates of various isotopes in copper at sea level. Calculations have carried out with GEANT4 [10], ACTIVIA [10], a standalone code [21] with spectrum from Ref. [8] and TALYS [19] cross-sections. The measurements have been reported in Refs. [22, 23]. The results reported in Ref. [22] for about 985 m above sea level with 20 g/cm^2 roof shielding were scaled down by a factor of 2.4 as suggested in Ref. [22]. Only neutrons above 4 MeV contribute to the activation at the surface because of the high threshold of reactions involved.

Table 1 reveals that the differences exist not only between measurements and calculations or calculations with difference codes, but also between the two measurements for some radioactive isotopes. The difference between the codes can be explained by different cross-sections and, sometimes, by different cosmic-ray spectra used. The difference between two or more experiments is harder to explain.

By comparing production rates by neutrons and protons, it is apparent that protons contribute no more than 10% to the total rate. This is consistent with the fraction of proton at energies below 1 GeV in cosmic rays at sea level.

Recent calculations of activation in stainless steel using GEANT4 and ACTIVIA have been reported in Ref. [10] and the measurements have been described in [22]. Here again significant differences between the codes are observed and none of the codes explains all available data. Given that titanium is now widely used for manufacturing cryostats for low-temperature experiments, whereas xenon is one of the most promising targets (active media) for dark matter and double-beta decay searches, the calculations of the activation of titanium and xenon have been carried out in Ref. [10] and compared (where possible) to the measurements from LUX [24] (after 90 days cooling down) and Ref. [23]. The measurement of the decay rate of ^{127}Xe reported in Ref. [24] agrees well with GEANT4 calculations from Ref. [10] and is higher that ACTIVIA predictions for both neutron spectra. For ^{133}Xe the measured decay rate is higher than predictions from both codes. Table 2 shows the calculation of xenon activation with GEANT4 and ACTIVIA from Ref. [10] and the measurements reported in Ref. [23].

TABLE 2. Calculated and measured production rates of radioactive isotopes in xenon at sea level. The rates are given in kg^{-1} day^{-1}. The two columns for ACTIVIA show calculations with two neutron spectra: from Refs. [6, 7] and from Ref. [8]. In both cases the default semi-empirical cross-sections have been used.

Isotope	Half-life days	GEANT4	ACTIVIA [6, 7]	ACTIVIA [8]	TALYS [21]	Data [23]
$^{127}_{54}$Xe	36.4	233	35.7	89.9		162 ± 24
$^{113}_{50}$Sn	115.1	6.90	4.39	5.89		< 4.8
$^{125}_{51}$Sb	986	1.48	0.016	0.009	0.5	51 ± 21

TABLE 3. Measured and calculated production rates of radioactive isotopes in germanium at sea level [25]. The rates are given in kg^{-1} day^{-1}. The two columns for ACTIVIA correspond to two different cross-sections, from Ref. [14, 15] and Ref. [17]. The results for ^{68}Ge have additional uncertainty due to the lack of knowledge of the history (activation) of Ge powder prior to crystallisation.

Isotope	Half-life days	Data [25]	ACTIVIA [14, 15]	ACTIVIA [17]	GEANT4 [10]	TALYS [21]	Data [26]	Data [27]
$^{3}_{1}$H	4500	82 ± 21	46	43.5	48.3	27.7		
$^{49}_{23}$V	330	2.8 ± 0.6	1.9	1.9				
$^{65}_{30}$Zn	244	106 ± 13	38.7	65.8		37.1		38 ± 6
$^{55}_{26}$Fe	997	4.6 ± 0.7	3.5	4.0		8.6		
$^{68}_{32}$Ge	270.8	> 71	23.1	45		41.3	81.6	30 ± 7

The most dangerous isotope in the activation of titanium is $^{46}_{21}$Sc with 83.8 day half-life. ^{46}Sc is produced in titanium through the reaction ^{46}Ti$(n, p)^{46}$Sc. LUX has performed an experiment by activating a sample of Ti (previously stored underground) at an elevated level of 1.5 km (3.4 times higher neutron flux compared to the sea level) for 6 months and measuring the decay rate of ^{46}Sc. The measurement show the decay rate of 4.4 ± 0.3 mBq/kg [24] compared to the GEANT4 and ACTIVIA predictions of 7.3, 2.9 and 7.3 mBq/kg, respectively (the two values from ACTIVIA show the results with the two neutron spectra from Refs. [6, 7], respectively).

Recent measurement of activation of natural Ge crystals has been reported in Ref. [25]. Table 3 shows the comparison of these measurements with other data and calculations. Note that a small difference in the results of different calculations with the same code may arise depending on whether the data for the neutron spectrum or the parameterisation of (the fit to) the data are used.

New measurements of activation of NaI have been carried out within the framework of the ANAIS project [28] and compared to the calculations using different cross-section (excitation function) libraries and the neutron spectrum from [8]. As in other experiments, there is no single code/library found that would explain the decay rates of all isotopes.

Other recent results on activation include studies of background in the CRESST-II dark matter experiment, including activation [29], irradiation of tellurium with high-energy neutrons and measurements of activation [30], and measurements of activation of lead using fast neutrons at LANSCE [31].

Activation of materials by natural radiation underground is highly suppressed compared to the surface. The flux of atmospheric hadrons is reduced by 3 orders of magnitude by a few metres of rock leaving only muons and their secondary particles (mainly hadrons) as potential sources of cosmogenic activation. The flux of muons decreases with depth and should not produce a significant number of radioactive isotopes although some experiments may be affected (see recent measurements by KamLAND [32] and Borexino [33]). Radiative neutron capture may also contribute to activation since the flux of thermal neutrons underground (after moderation on light targets) exceeds that of very high-energy neutrons capable to activate materials. Special caution should be paid to neutron sources used for detector calibration. Although usually these sources have energies below 10 MeV and hence, below the threshold of most activation reactions, thermalised neutrons may be responsible for the radioactive isotope production and these effects have not been fully studied.

CONCLUSIONS

Cosmogenic activation of materials becomes more or more important with the increase of detector sensitivity. We may not have full (and accurate) knowledge of this yet. Several codes exist to calculate production rates but they do not provide consistent results. Neutron spectra and excitation functions (cross-sections) are important for calculating production rates of radio-isotopes and they are not well known (different libraries give different results). Measurements should provide key figures, also for tuning the codes but require knowledge of the material (exposure) history. There is no consistent picture of what code is better: different codes tend to better match data from different targets. We all hope to achieve progress here for better assessing the requirements for future experiments. For some experiments activation of detector components during calibration with neutron sources may also become important but this requires further studies for specific materials and experimental setups.

REFERENCES

[1] S. Cebrian *et al.*, Journal of Physics, Conference series **39**, p. 344 (2006).
[2] S. Cebrian *et al.*, Astroparticle Physics **33**, p. 316 (2010).
[3] S. Cebrian, American Institute of Physics, Conference series **1549**, p. 136 (2013).
[4] C. Patrignani *et al.*, (Particle Data Group) Review of particle physics, Chin. Phys. C **40**, p. 1 (2016).
[5] J. J. Back and Y. A. Ramachers, Nucl. Instrum. and Meth. in Phys. Res A **586**, p. 286 (2008).
[6] T. W. Armstrong, K. C. Chandler, and J. Barish, J. Geophys. Res. **78**, p. 2715 (1973).
[7] N. Gehrels, Nucl. Instrum. and Meth. in Phys. Res A **239**, p. 324 (1985).
[8] M. S. Gordon *et al.*, IEEE Transactions on Nuclear Science **51**, p. 3427 (2004).
[9] V. Lozza and J. Petzoldt, Astroparticle Physics **61**, p. 62 (2015).
[10] C. Zhang, D.-M. Mei, V. A. Kudryavtsev, and S. Fiorucci, Astroparticle Physics **84**, p. 62 (2016).
[11] J. F. Ziegler, IBM J. Res. Develop. **42**, p. 117 (1998).
[12] C. Hagmann, D. Lange, and D. Wright, IEEE Nuclear Science Symposium NS24–36 (2007).
[13] T. Blackwell, "The use of cosmic-rays in detecting illicit nuclear materials," Ph.D. thesis, University of Sheffield 2015.
[14] R. Silberberg and C. Tsao, Physics Reports **191**, p. 351 (1990).
[15] R. Silberberg, C. H. Tsao, and A. F. Barghouty, Astrophys. J. **501**, p. 911 (1998).
[16] Y. N. Shubin *et al.*, IAEA-NDS-136 (1995).
[17] Y. N. Shubin *et al.*, IAEA-NDS- 204 (1998).
[18] C. J. Martoff and P. D. Lewin, Comput. Phys. Commun. **72**, p. 96 (1992).
[19] A. J. Koning and D. Rochman, Nuclear Data Sheets **113**, p. 2841 (2012).
[20] S. Agostinelli *et al.*, Nucl. Instrum. and Meth. in Phys. Res A. **506**, p. 250 (2003).
[21] D.-M. Mei, Z.-B. Yin, and S. Elliott, Astroparticle Physics **31**, p. 417 (2009).
[22] M. Laubenstein and G. Heusser, Applied Radiation and Isotopes **67**, p. 750 (2009).
[23] L. Baudis *et al.*, European Physical Journal **75**, p. 485 (2015).
[24] D. S. Akerib *et al.*, Astroparticle Physics **62**, p. 33 (2015).
[25] E. Armengaud *et al.*, Astroparticle Physics **91**, p. 51 (2017).
[26] I. Barabanov *et al.*, Nucl. Instrum. Meth. in Phys. Res. B **251**, p. 115 (2006).
[27] F. T. Avignone *et al.*, Nucl. Phys. B (Proc. Suppl.) **28A**, p. 280 (1992).
[28] J. Amare *et al.*, JCAP **02**, p. 046 (2015).
[29] R. Strauss *et al.*, JCAP **06**, p. 030 (2015).
[30] B. S. Wang *et al.*, Phys. Rev. C **92**, p. 024620 (2015).
[31] V. E. Guiseppe *et al.*, Astroparticle Physics **64**, p. 34 (2015).
[32] S. Abe *et al.*, Phys. Rev. C **81**, p. 025807 (2010).
[33] G. Bellini *et al.*, JCAP **1308**, p. 049 (2013).